Eur. Phys. J. B **28**, 475–481 (2002)
DOI: 10.1140/epjb/e2002-00250-6

THE EUROPEAN PHYSICAL JOURNAL B

Electron energy state spin-splitting in 3D cylindrical semiconductor quantum dots

Y. Li[1,2,a], Voskoboynikov[3,4], C.P. Lee[3], S.M. Sze[1,3], and O. Tretyak[4]

[1] National Nano Device Laboratories, Hsinchu 300, Taiwan
[2] Microelectronics and Information Systems Research Center, National Chiao Tung University, Hsinchu 300, Taiwan
[3] Institute of Electronics, National Chiao Tung University, Hsinchu 300, Taiwan
[4] Kiev Taras Shevchenko University, 01033, Kiev, Ukraine

Received 15 May 2001 / Received in final form 14 May 2002
Published online 13 August 2002 –

Abstract. In this article we study the impact of the spin-orbit interaction on the electron quantum confinement for narrow gap semiconductor quantum dots. The model formulation includes: (1) the effective one-band Hamiltonian approximation; (2) the position- and energy-dependent quasi-particle effective mass approximation; (3) the finite hard wall confinement potential; and (4) the spin-dependent Ben Daniel-Duke boundary conditions. The Hartree-Fock approximation is also utilized for evaluating the characteristics of a two-electron quantum dot system. In our calculation, we describe the spin-orbit interaction which comes from both the spin-dependent boundary conditions and the Rashba term (for two-electron quantum dot system). It can significantly modify the electron energy spectrum for InAs semiconductor quantum dots built in the GaAs matrix. The energy state spin-splitting is strongly dependent on the dot size and reaches an experimentally measurable magnitude for relatively small dots. In addition, we have found the Coulomb interaction and the spin-splitting are suppressed in quantum dots with small height.

PACS. 71.70.Ej Spin-orbit coupling, Zeeman and Stark splitting, Jahn-Teller effect – 73.21.La Quantum dots – 78.20.Bh Theory, models, and numerical simulation – 85.35.Be Quantum well devices (quantum dots, quantum wires, etc.)

1 Introduction

The study of semiconductor quantum dots has been of great interests [1–4] in recent years. These "artificial atoms" are the most attractive because of their applications in micro and nano optical electronics [5–7]. From this point of view, the hierarchical structure of the electron energy states in semiconductor quantum dots is an important object to be studied.

The electron spin plays a crucial role in the design of electron energy states in semiconductor quantum dots [8]. In spintronics, which is a new promising branch of the electronics, the spin-dependent energy structure for semiconductor quantum dots can be an important factor [9,10]. The spin-orbit interaction is one of possible opportunities to control the electron spin in a complete semiconductor system. It has been found recently that the spin-orbit interaction has an evident impact upon the energy states and electronic properties for various III-V semiconductor quantum heterostructures [11–14], but the effects of the spin-orbit interaction for semiconductor quantum dots have been investigated for simple two-dimensional (2D) models [15] and still do not have a good understanding.

A wide range of theoretical calculations has been done to simulate electronic properties of quantum dots and most of them use numerical methods. The energy level calculation has been done using the effective-mass approximation with [16–23] and without [24–27] the coordinate dependence. The multiband $\mathbf{k} \cdot \mathbf{p}$ method with finite [28–30] or infinite [30,31] confinement potentials and pseudopotential self-consistent methods were used in the simulations ([32,33] and references therein).

In this work, we concentrate on the impact of the spin-orbit interaction for the electron quantum confinement in small three-dimensional (3D) cylindrical InAs quantum dots embedded into GaAs matrix. We formulate the problem that based on: (1) the effective electronic one band Hamiltonian; (2) the energy- and position-dependent electron effective mass approximation; and (3) the spin-dependent Ben Daniel-Duke boundary conditions [11] simultaneously; then we solved numerically. In addition, we use a realistic hard wall (of finite barrier height) 3D confinement potential for quantum dots which are disk shape with the radius R_0 and height z_0. The potential is induced

[a] e-mail: ymli@cc.nctu.edu.tw

by the discontinuity of the conduction band between the interface of the quantum dot. The spin-dependent boundary conditions are generated by the difference of spin-orbit interaction parameters between the quantum dot and the semiconductor matrix. We calculated the single electron energy states and two-electron ground state energy in small dots. For the single electron model, the spin-splitting boundary condition lead to a spin-spliting in the single electron energy states. The two-electron charge potential generates an additional part of the spin-orbit interaction for an electron moving in the two-electron charge potential [11], and then it produces an additional (Rashba type) spin-splitting.

We generalize the nonlinear iterative method to solve the 3D nonlinear Schrödinger equation. This nonlinear iterative method has been proposed by us earlier to compute the electronic states of semiconductor quantum dots [34–37]. In each iteration loop, a balanced- and shifted-QR algorithm and the inverse iteration method are applied to calculate the corresponding eigenvalues and eigenvectors of the discretized Schrödinger equation [38–43]. Our calculation results suggest the spin-orbit interaction can significantly modify the electron energy spectrum of InAs/GaAs semiconductor quantum dots. For a single electron system, we have found that the spin-dependent boundary conditions contribute a sizable spin-splitting of the electron energy states for exciting states. The spin-splitting for the lowest single electron energy states demonstrates a strong dependence on the dot size and it reaches an experimentally measurable magnitude for the relatively small quantum dots.

The two-electron problem has been solved by the restricted Hartree-Fock method [44,45]. The electron-electron interaction leads to a small Coulomb correction of the ground state energy. In addition, the Rashba spin-splitting is essentially smaller than that generated by the spin-dependent boundary conditions. In our realistic 3D quantum dot model, we found that an anomalous scaling of the Coulomb interaction energy decreases as the dot height decreases. It can be considered as a direct result of the electron wave function localization properties for 3D systems with the finite confinement potential [32,33].

This paper is organized as follows. Section 2 provides the quantum dot model description for a single electron system. Section 3 states the model for two-electron system. Section 4 is devoted to the description of calculation methods. Section 5 presents the computational results and discussions. Section 6 draws the conclusions and suggests the future works and remarks.

2 A single electron system

Considering an electron confined in a 3D quantum dot and applying an effective one electronic band Hamiltonian, we have [11]

$$\hat{H}_{se} = \hat{H}_0 + \hat{V}_{so}(\mathbf{r}), \tag{1}$$

where $\hat{H}_0$ is the Hamiltonian of the system without spin-orbit interaction and $V_{so}(\mathbf{r})$ indicates the spin-orbit interaction for electrons in the conduction band. The expression of $\hat{H}_0$ is as follows [46]:

$$\hat{H}_0 = -\frac{\hbar^2}{2}\nabla_{\mathbf{r}}\left(\frac{1}{m(E,\mathbf{r})}\right)\nabla_{\mathbf{r}} + V(\mathbf{r}), \tag{2}$$

where $\nabla_{\mathbf{r}}$ stands for the spatial gradient. The $m(E,\mathbf{r})$ is the energy- and position-dependent electron effective mass

$$\frac{1}{m(E,\mathbf{r})} = \frac{2P^2}{3\hbar^2}\left[\frac{2}{E+E_g(\mathbf{r})-V(\mathbf{r})} + \frac{1}{E+E_g(\mathbf{r})+\Delta(\mathbf{r})-V(\mathbf{r})}\right], \tag{3}$$

where $V(\mathbf{r})$ is the confinement potential, P is the momentum matrix element, and $E_g(\mathbf{r})$ and $\Delta(\mathbf{r})$ are the position-dependent band gap and the spin-orbit splitting in the valence band, respectively. The spin-orbit interaction for the conduction band electrons, $V_{so}(\mathbf{r})$ is given by [47]

$$\hat{V}_{so}(\mathbf{r}) = \mathrm{i}\nabla\beta(E,\mathbf{r})\cdot[\widehat{\sigma}\times\nabla], \tag{4}$$

where $\beta(E,\mathbf{r})$ is the spin-orbit coupling parameter, and $\widehat{\sigma}=\{\sigma_{\mathbf{x}},\sigma_{\mathbf{y}},\sigma_{\mathbf{z}}\}$ is the vector of the Pauli matrices. The energy- and position-dependent $\beta(E,\mathbf{r})$ has the form as

$$\beta(E,\mathbf{r}) = \frac{P^2}{3}\left[\frac{1}{E+E_g(\mathbf{r})-V(\mathbf{r})} - \frac{1}{E+E_g(\mathbf{r})+\Delta(\mathbf{r})-V(\mathbf{r})}\right]. \tag{5}$$

For the quantum dot system with the sharp discontinuity on the conduction band interfaces between the quantum dot (material 1) and semiconductor matrix (material 2), the hard-wall confinement potential is

$$V(\mathbf{r}) = \begin{cases} 0, & \mathbf{r}\in \text{material 1} \\ V_0, & \mathbf{r}\in \text{material 2}, \end{cases} \tag{6}$$

where V_0 is the band offset of structures. Combining the Hamiltonian in equations (1, 2), and (4), and taking an integration of this Schrödinger equation with respect to the direction perpendicular to the system interface, the spin-dependent Ben Daniel-Duke boundary conditions for the electron wave function $\Psi(\mathbf{r})$ is written as follows:

$$\begin{aligned} &\Psi_{\text{material 1}}(\mathbf{r}_s) = \Psi_{\text{material 2}}(\mathbf{r}_s) \\ &\left\{\tfrac{\hbar^2}{2m(E,\mathbf{r}_s)}\nabla - \mathrm{i}\beta(E,\mathbf{r}_s)[\widehat{\sigma}\times\nabla]\right\}_n \Psi(\mathbf{r}_s) = C_0, \end{aligned} \tag{7}$$

where C_0 is a constant, and $\mathbf{r}_s$ denotes the position of the system interface.

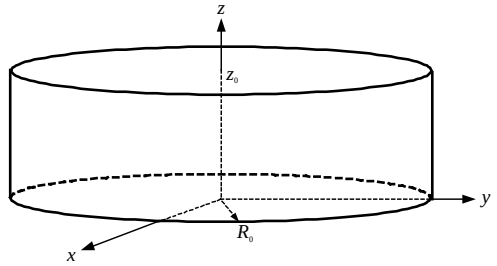

Fig. 1. A schematic diagram for the disk-shaped quantum dot.

We now consider a disk-shaped semiconductor quantum dot (see Fig. 1) with the radius R_0 and height z_0 in the cylindrical coordinate (R, ϕ, z). The origin of the system is at the center of the disk, and the z axis is chosen along the rotation axis. Since the system is cylindrically symmetric, the wave function can be represented as

$$\Psi_l(\mathbf{r}) = \Phi_l(R, z)\exp(\mathrm{i}l\phi), \tag{8}$$

where $l = 0, \pm1, \pm2, ...$ is the electron orbital quantum number, and the original model remains a 2D problem in the $(R,\ z)$ coordinate. From equations (1–6) and (8), we obtain equations

$$-\frac{\hbar^2}{2m_1(E)}\left(\frac{\partial^2}{\partial R^2} + \frac{\partial}{R\partial R} + \frac{\partial^2}{\partial z^2} - \frac{l^2}{R^2}\right)\Phi_{l1}(R,z) =$$

$$E\Phi_{l1}(R,z),\ R \le R_0,\ |z| \le \frac{z_0}{2} \tag{9}$$

$$-\frac{\hbar^2}{2m_2(E)}\left(\frac{\partial^2}{\partial R^2} + \frac{\partial}{R\partial R} + \frac{\partial^2}{\partial z^2} - \frac{l^2}{R^2}\right)\Phi_{l2}(R,z)$$
$$+ V_0\Phi_{l2}(R,z) = E\Phi_{l2}(R,z),\ R > R_0,\ |z| > \frac{z_0}{2}\cdot \tag{10}$$

With the same reasons that the problem is symmetric along the z axis, the spin-dependent boundary conditions in equation (7) are given by

$$\Phi_{l1}(R_0,z) = \Phi_{l2}(R_0,z),\ |z| \le \frac{z_0}{2} \tag{11}$$

$$\Phi_{l1}(R,\pm\frac{z_0}{2}) = \Phi_{l2}(R,\pm\frac{z_0}{2}),\ R \le R_0 \tag{12}$$

$$\frac{1}{m_1}\left.\frac{\partial\Phi_{l1}(R,z)}{\partial R}\right|_{R_0} - \frac{1}{m_2}\left.\frac{\partial\Phi_{l2}(R,z)}{\partial R}\right|_{R_0}$$

$$+\frac{2\sigma(\beta_1-\beta_2)}{\hbar^2}\frac{l}{R_0}\Phi_{l1}(R_0,z) = 0,\ |z| \le \frac{z_0}{2} \tag{13}$$

$$\left.\frac{1}{m_1}\frac{\partial\Phi_{l1}(R,z)}{\partial z}\right|_{\pm\frac{z_0}{2}} - \left.\frac{1}{m_2}\frac{\partial\Phi_{l2}(R,z)}{\partial z}\right|_{\pm\frac{z_0}{2}} = 0,\ R \le R_0, \tag{14}$$

where σ refers to the electron spin polarization along the z axis. Both the electron energy state and wave functions are tightly coupled and complicated with the quantum dot parameters and the electron angular momentum. We solve equations (9, 10) with their boundary conditions (11–14) using the proposed numerical methods in Section 4.

In the discrete energy spectrum of the quantum dot, the energy states are numerated by a set of numbers $\{n, l, \sigma\}$, where n is the nth solution of the problem with the fixed l and σ. For the same value of n, the parallel (or antiparallel) orbital momentum, and spin, the energy states still have two-fold degeneration (well-known Kramers degeneracy). However, the nth state with antiparallel orbital momentum and spin are separated from the n-th state with parallel orbital momentum and spin.

In the cylindrical quantum dot, a conventional notation nL_σ for the electron energy states is adopted, where $L = S, P, D, ...$ denotes the absolute value of l, and $\sigma = \pm1$ refers to the electron spin directions corresponding to the electron angular momentum direction. For all calculations we choose the lowest energy state ($n = 1$). The spin-splitting energy is defined as

$$\Delta E_{nL} = E_{nL_{+1}} - E_{nL_{-1}}. \tag{15}$$

The two-electron charge potential has an additional part of the spin-orbit interaction with the Rashba term. The problem of the two-electron system is solved by the restricted Hartree-Fock method in the next section.

3 A two-electron system

The Hamiltonian describing the system of two-electron interaction is given by [44,48]

$$\hat{H} = \sum_{i=1,2}\hat{H}^i_{se} + V_C(\mathbf{r}^1,\mathbf{r}^2) + \hat{V}_R, \tag{16}$$

where H^i_{se} represents the effective Hamiltonian as shown in equation (1) for the ith electron, $V_C(r_1, r_2)$ is the Coulomb repulsion among the electrons, and V_R is the spin-orbit interaction of an electron moving in the Coulomb repulsion potential

$$\hat{V}_R = -\mathrm{i}\sum_{i=1,2}\sum_{j\neq i}\alpha(\mathbf{r}^i)\nabla^i V_C(\mathbf{r}^i,\mathbf{r}^j)\cdot\left[\widehat{\sigma}^i\times\nabla^i\right], \tag{17}$$

where α is the Rashba spin-orbit coupling parameter [47]. The expression of α is as follows

$$\alpha(\mathbf{r}) = \frac{\hbar^2}{2m(0,\mathbf{r})}\frac{\Delta(\mathbf{r})}{E_g(\mathbf{r})}\frac{2E_g(\mathbf{r})+\Delta(\mathbf{r})}{[E_g(\mathbf{r})+\Delta(\mathbf{r})]\,[3E_g(\mathbf{r})+\Delta(\mathbf{r})]}\cdot \tag{18}$$

The Coulomb repulsion $V_C(r_1, r_2)$ is defined as [49]

$$V_C(\mathbf{r}^1, \mathbf{r}^2) = \frac{1}{4\pi\varepsilon_0\overline{\varepsilon}\,|\mathbf{r}^1 - \mathbf{r}^2|},$$

where ε_0 is the permittivity of vacuum and $\overline{\varepsilon} = (\varepsilon_1+\varepsilon_2)/2$ is the average dielectric constant, which introduces only a small error for InAs/GaAs quantum dot systems since the dielectric constant ε_1 and ε_2 differ by less then 13%.

In the restricted Hartree-Fock approximation [44,45,48], when the two electrons are in the ground state of $(1S_{+1}) + (1S_{-1})$ configuration, we can consider the spatial wave function of the ground state ($l^1 = l^2 = 0$) as

$$U(\mathbf{r}^1, \mathbf{r}^2) = u(\mathbf{r}^1)u(\mathbf{r}^2), \tag{19}$$

where $u(\mathbf{r}_i)$ is the normalized to unity solution of the differential-integral equation in the form

$$\left[H^i_{se} + G(\mathbf{r}^i) - E^i\right] u(\mathbf{r}^i) = 0, \tag{20}$$

with

$$G(\mathbf{r}^i) = \int \frac{\left|u(\mathbf{r}^j)\right|^2 \mathrm{d}\mathbf{r}^j}{4\pi\varepsilon_0\overline{\varepsilon}\,|\mathbf{r}^i - \mathbf{r}^j|}\,. \tag{21}$$

The expectation value of the ground state energy (since the solutions 1 and 2 are identical) is

$$\bar{E} = 2E^1 - \bar{G}, \tag{22}$$

where

$$\bar{G} = \int G(\mathbf{r}^1)\left|u(\mathbf{r}^1)\right|^2 \mathrm{d}\mathbf{r}^1.$$

The electron addition energy [8,33] in our system is

$$\Delta(1) = \bar{E} - E_{1S_{\pm1}}. \tag{23}$$

Within the restricted Hartree-Fock approximation, we evaluate an addition spin-splitting ΔE^R_{1L}. It comes with the Rashba term which is generated by the charge of "the core electron" (ground state), and can be calculated as

$$\Delta E^R_{1L} = E^R_{1L_{+1}} - E^R_{1L_{-1}}, \tag{24}$$

where

$$E^R_{1L_{\pm1}} = -2\mathrm{i}\int \alpha(\mathbf{r})\Psi^*_l(\mathbf{r})\chi^*_{\pm1}\nabla G(\mathbf{r})\left[\widehat{\sigma}\times\nabla\right]\Psi_l(\mathbf{r})\chi_{\pm1}\mathrm{d}\mathbf{r},$$

and χ_σ is a spin function upon which the Pauli matrix vector operates

$$\chi_{+1} = \begin{pmatrix}1\\0\end{pmatrix},\ \chi_{-1} = \begin{pmatrix}0\\1\end{pmatrix}. \tag{25}$$

4 Method of calculation

To solve the nonlinear Schrödinger equation, we generalize here the nonlinear iterative scheme proposed by us earlier [34–37]. This novel solution scheme for the single electron system simulation consists of steps: (i) set initial energy; (ii) compute electron effective mass; (iii) compute spin-orbit coupling parameter; (iv) solve the Schrödinger equation; and (v) update the newer energy and back to step (ii). The iteration will be terminated when the computed energy is converged to a specified tolerance error. Once the convergent results are obtained, we perform the post process to calculate the spin-splitting energy and related quantities.

For the two-electron system simulation, we have also developed a similar nonlinear iteration algorithm. The algorithm is outlined as follows: (a) set initial parameters and estimate an initial energy, (b) compute the electron effective mass, (c) compute the spin-orbit coupling parameter, (d) compute the Coulomb repulsion potential, (e) solve the corresponding Schrödinger equation, and (f) update the newer energy and back to step (b). The iteration terminates when the desired energy is convergent.

To obtain the complete numerical solution of the Schrödinger equation in step (iv) or (e) above, a finite difference method with nonuniform mesh technique is firstly applied to discretize the Schrödinger equation [38]. The discretized Schrödinger equation with its boundary conditions leads to an algebraic eigenvalue problem as follows

$$A\mathbf{X} = \lambda\mathbf{X}, \tag{26}$$

where A is the matrix arising from the discretized Schrödinger equation and boundary conditions, $\mathbf{X}$, and λ to be computed are the corresponding eigenvectors (wave functions) and the eigenvalues (energy states) of the matrix A, respectively. Because the matrix A is an energy-dependent, five-diagonal, nonsymmetric, and large sparse matrix, the eigenvalues of such matrix can be very sensitive to small changes in the matrix elements [39–41]. One of the main reasons resulting in the sensitivity of eigenvalues of the matrix A is the discontinuity between the interface and the rest part of quantum dots. It directly affects the intrinsic property of the matrix A by introducing some extreme elements. Therefore, we apply the balanced algorithm [39–41] to reduce the sensitivity of eigenvalues of the matrix A to small changes in the matrix elements. Then the balanced matrix A is transformed into a simpler upper Hessenberg form. The eigenvalues of the upper Hessenberg matrix are directly computed with the shifted-QR method [39,40]. The shifted- and balanced-QR method is the dominant method for solving nonsymmetric matrix eigenvalue problem [42]. When an eigenvalue is found, the corresponding eigenvector of this eigenvalue is calculated with the inverse iteration method [39,43].

According to our calculation experience, the applied nonlinear iterative method converges monotonically for the simulation of both the single electron system and the

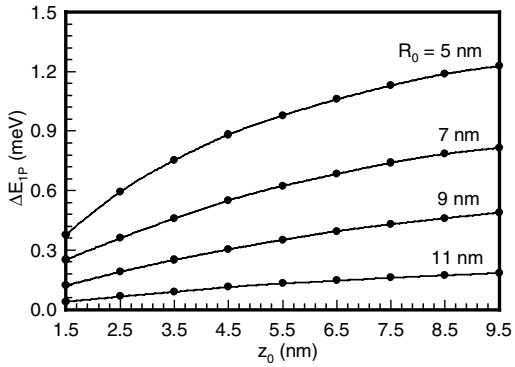

Fig. 2. The dependence of the $1P$ energy state splitting on the dot size.

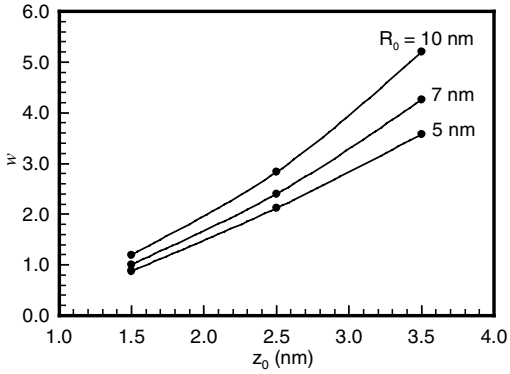

Fig. 3. The ratio w for various dot sizes ($n = 1, l = 1, \sigma = -1$).

two-electron system at the same time. A strict convergence criterion on energies (the maximum norm error is less than 10^{-8} eV) can be reached by taking only 9–10 (or 12–13) feedback nonlinear iterations for the single electron system (or the two-electron system).

5 Results and discussions

In the calculation of the single electron energy spectra for InAs cylindrical quantum dots in GaAs matrix, the following semiconductor band structure parameters are used. For the InAs, the energy gap E_{1g} is 0.42 eV, spin-orbit splitting Δ_1 is 0.42 eV, the value of the nonparabolicity parameter E_{1p} is $3m_0P_1^2/\hbar^2 = 22.2$ eV, and m_0 is the free electron effective mass. For the GaAs we choose $E_{2g} = 1.52$ eV, $\Delta_2 = 0.34$ eV, and $E_{2p} = 24.2$ eV. The band offset is taken as $V_0 = 0.77$ eV [46]. The spin-splitting effect is obviously equal to zero for the lowest energy state $1S_{\pm 1}$. The dependence of the $1P$ energy state splitting, ΔE_{1P}, on the quantum dot size is shown in Figure 2 for various sizes of quantum dots.

This theory demonstrates an evident spin-splitting of the $1P$ energy state for small quantum dots. The splitting is strongly dependent on the dot radius and it decreases when the dot radius increases. At the same time, for quantum dots with small height the spin-splitting is small. As shown in Figure 2, there is a 1.0 meV difference in ΔE_{1P} for z_0 varies from 1.5 nm to 9.5 nm when the dot radius is fixed at 5.0 nm. This is a result of the electron wave function tunneling into the barrier along the z axis.

To clarify this effect, we compare probabilities to find the electron inside and outside the dot by examining the following occupancy-ratio

$$w = \frac{\int_{r\in\text{material 1}} \mathrm{d}\mathbf{r}^3 |\Phi(R,z)|^2}{\int_{r\in\text{material 2}} \mathrm{d}\mathbf{r}^3 |\Phi(R,z)|^2}\,. \tag{27}$$

As shown in Figure 3, for the quantum dots with a small height, the electron wave function spreads out of the quantum dot ($w \sim 1$), and the property of the energy state is controlled by the band parameters of GaAs matrix. In this situation an effective difference of spin-orbit coupling parameters $\beta_1 - \beta_2$ is rather small. When z_0 increases, the difference also increases and then becomes independent

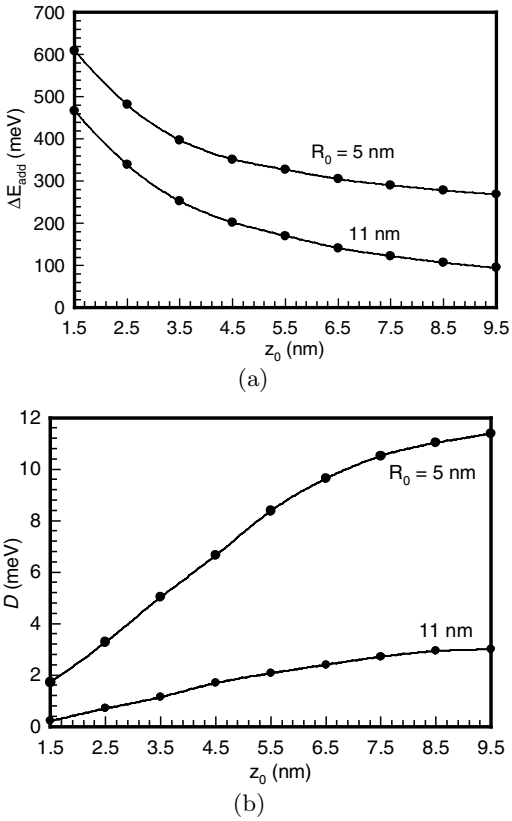

Fig. 4. (a) The addition energy ΔE_{add} of dots. (b) The difference $D = \Delta(1) - E_{1S_{\pm 1}}$ for various dot sizes.

on z_0. For a fixed z_0, the more R_0 increases, the smaller energy of the electron bound states becomes and it provides the smaller penetration of the electron wave function into the barrier. This makes the energy splitting large for the cylindrical quantum dots with the small height.

The electron addition energy depending on the dot size is calculated by equations (22–24) and the scheme described above. We found that the addition energy is slightly different from the single electron ground state. The addition energy of dots and the difference, $D = \Delta(1) - E_{1S_{\pm 1}}$, (representing the Coulomb interaction impact onto the energy state for various dot sizes) are shown in Figures 4a and b, respectively. We have two observations. First, the one electron addition energy in the InAs

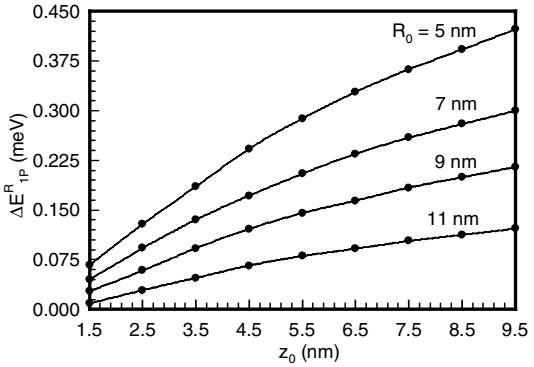

Fig. 5. The spin-splitting ΔE^R_{1P} of the Rashba term.

quantum dots increases as the dot size decreases rapidly. Second, the dependence of the dot height for the Coulomb part of the addition energy D does not follow the conventional scheme; it decreases when the dot height decreases. The last observation is contrary to the conventional point of view [50]. This result is the direct consequence of the parameter w depending on the dot size; in other words, the wave function spreading enhances the characteristic size of the dot and effectively decreases the Coulomb interactions. It should be noticed that the addition energy is an experimentally measurable quantity [8]. By comparing with the one electron energy in the dot, it provides us more information about D than it about the Coulomb interaction of few electrons in small quantum dots.

As shown in Figure 5, we present the spin-splitting, ΔE^R_{1P}, of the Rashba term. It follows the observation described above (*i.e.*, the addition splitting decreases as the dot height decreases). Furthermore, it is sufficiently smaller than the splitting comes from the spin-dependent boundary conditions. The total spin-splitting, $\Delta E_{1P} + \Delta E^R_{1P}$, produces a measurable quantity for the infrared optical experiment.

Before we conclude, we would like to mention that an experimental observation of the effects described above requires some specific conditions. First of all the dots should be really small (lateral size about 10 nm) and highly homogeneous in sizes. It is also interesting to study a local small single dot system [51]. Satisfying those conditions, one can use any spectroscopic technique elaborated in the quantum dot investigations ([8,52,53] and reference therein). To our best knowledge, such kind of experiments for InAs/GaAs quantum dots has not been done yet.

6 Conclusions

We have studied the impact of the spin-orbit interaction on the electron energy states for small semiconductor cylindrical quantum dots. We formulated and solved the 3D problem with (1) the effective one electronic band Hamiltonian, (2) the energy- and position-dependent electron effective mass and (3) the spin-dependent Ben Daniel-Duke boundary conditions for quantum dots with various sizes. The restricted Hartree-Fock approximation has been also utilized to evaluate the characteristics of a two-electron quantum dots.

Our calculation results demonstrate that the spin-orbit interaction comes both from the spin-dependent boundary conditions and the Rashba term (for two-electron quantum dot system). It can significantly modify the electron energy spectrum of the InAs semiconductor quantum dots built in the GaAs matrix. The splitting is strongly dependent on the quantum dot size and reaches an experimentally measurable magnitude for relatively small quantum dots. In addition, we have found that the Coulomb interaction and the spin-splitting can be suppressed in quantum dots with small height.

We would like to point out that the model, simulation methods, and results presented here can be used as a starting point in the estimation of the spin-orbit interaction effects in 3D semiconductor quantum dots. Future calculations include a self-consistent potential and the multiband approach to obtain proper quantitative results.

The authors express their appreciation to the referee for an exceptional in-depth reading of the manuscript. This work was supported in part by the National Science Council of Taiwan under contract No. NSC 90-2112-M-317-001 and 90-2215-E-009-025.

References

1. R. Pino, Eur. Phys. J. B **13**, 723 (2000)
2. J. Kolehmainen, *et al.*, Eur. Phys. J. B **13**, 731 (2000)
3. K. Maschke, *et al.*, Eur. Phys. J. B **19**, 599 (2001)
4. D. Bimberg, Semicond. **33**, 951 (1999)
5. D. Bimberg, *et al.*, Thin Solid Films **367**, 235 (2000)
6. N.N. Ledentspin-orbitv, *et al.*, Semicond. **32**, 343 (1998)
7. E. Tpwe, D. Pan, IEEE J. Selec. Top. Quantum Electron. **6,** 408 (2000)
8. S. Tarucha, T. Honda, D.C. Austing, *et al.*, Physica E **3**, 112 (1998)
9. X. Hu, S. Das Sarma, Phys. Rev. A **61**, 062301 (2000)
10. S. Bandyopadhyay, Phys. Rev. B **61**, 813 (2000)
11. E.A. de Andrada e Silva, G.C. La Rocca, F. Bassani, Phys. Rev. B **55**, 16293 (1997)
12. O. Voskoboynikov, *et al.*, J. App. Phys. **87**, 1 (2000)
13. A.G. Mal'shukov, K.A. Chao, Phys. Rev. B **61**, R2413 (2000)
14. P.N. Racec, *et al.*, Phys. Rev. B **56**, 3595 (1997)
15. O. Voskoboynikov, *et al.*, Phys. Rev. B **63**, 165306 (2001)
16. G. Lamouche, Y. Lépin, Phys. Rev. B **51**, 1950 (1995)
17. F.M. Peeters, V.A. Schweigert, Phys. Rev. B **53**, 1468 (1996)
18. P. Lelong, G. Bastard, Solid State Commun. **98**, 819 (1996)
19. D.M.T. Kuo, Y.C. Chang, Phys. Rev. B **61**, 11051 (2000)
20. N. Singh, Ranjan, V.A. Singh, Int. J. Mod. Phys. **14**, 1753 (2000)
21. M. Grudman, O. Stier, D. Bimberg, Phys. Rev. B **52**, 11969 (1995); Phys. Rev. B **59**, 5688 (1999)
22. M. Califano, P. Harrison, Phys. Rev. B **61,** 10959 (2000)
23. M. Califano, P. Harrison, J. Appl. Phys. **88**, 5870 (2000)

24. A. Wojs, P. Hawrylak, S. Fafard, L. Jasak, Phys. Rev. B **54**, 5604 (1996)
25. A.H. Rodríguez, C. Trallero-Giner, S.E. Ulloa, J. Marín-Antuña, Phys. Rev. B **63**, 125319 (2001)
26. J. Shumway, L.R.C. Fonseca, J.P. Leburton, R.M. Martin, D.M. Ceperley, Physica E **8**, 260 (2000)
27. S.S. Li, J.B. Xia, J. Appl. Phys. **84**, 3710 (1998)
28. M.A. Cusak, P.R. Briddon, M. Jaros, Phys. Rev. B **54**, R2300 (1996)
29. C. Prior, Phys. Rev. B **60**, 2869 (1999)
30. P.C. Sercel, K.J. Vahala, Phys. Rev. B **42**, 3690 (1990)
31. Al.L. Rosen, M. Rosen, Phys. Rev. B **58**, 7120 (1998)
32. A.J. Williamson, A. Zunger, Phys. Rev. B **59**, 15819 (1999)
33. A. Franceschetti, A. Zunger, Phys. Rev. B **62**, 2614 (2000)
34. Y. Li, *et al.*, J. Appl. Phys. **90**, 6416 (2001)
35. Y. Li, *et al.*, Comput. Phys. Commun. **141**, 66 (2001)
36. Y. Li, *et al.*, Comput. Phys. Commun. **140**, 399 (2001)
37. Y. Li, *et al.*, Solid State Commun. **120**, 79 (2001)
38. R.S. Varga, *Matrix Iterative Analysis* (Prentice-Hall, 2000)
39. J.H. Wilkinson, C. Reinsch, *Linear Algebra II of Handbook for Automatic Computation* (Springer-Verlag, 1971)
40. Y. Saad, *Numerical methods for large eigenvalue problems* (Manchester University Press, 1992)
41. B.N. Parlett, C. Reinsch, Numer. Math. **13**, 293 (1969)
42. D.S. Watkins, J. Comp. App. Math. **123,** 67 (2000)
43. I.C.F. Ipsen, SIAM Rev. **39**, 254 (1997)
44. H.A. Bethe, E.E. Salpeter, *Quantum Mechanics of One- and Two-Electron Atoms* (Plenum PC, 1977)
45. R.C. Parr, W. Yang, *Density-Functional Theory af Atoms and Molecules* (Oxford University Press, 1989)
46. G. Bastard, *Wave Mechanics Applied to Semiconductor Heterostructures* (Les Édition de Physique, Les Ulis, 1988)
47. Th. Schäpers, G. Engeles, J. Lange, *et al.*, J. Appl. Phys. **83**, 4324 (1998)
48. I. Lindgren, J. Morrison, *Atomic Many-Body Theory* (Springer-Verlag, 1985)
49. L.R. Fonceca, J.L. Jimenez, J.P. Leburton, R.M. Martin, Phys. Rev. B **57**, 4017 (1998)
50. F.A. Reboredo, A. Franceschetti, A. Zunger, Phys. Rev. B **61**, 13073 (2000)
51. P. Michler, A. Kiraz, Lidong Zhang, C. Becher, E. Hu, A. Imamoglu, App. Phys. Lett. **77**, 184 (2000)
52. P.M. Petroff, K.H. Schmidt, G.M. Ribeiro, A. Lorke, J. Kotthaus, Jpn J. Appl. Phys. **36**, 4068 (1997)
53. R.J. Warburton, B.T. Miller, C.S. Durr, C. Bodefeld, K. Karrai, J.P. Kotthaus, G. Medeiros-Ribeiro, P.M. Petroff, S. Huant, Phys. Rev. B **58**, 16221 (1998)